

# Learning Directed Graphical Models from Gaussian Data

Katherine Fitch\*

July 19, 2022

## Abstract

In this paper, we introduce two new directed graphical models from Gaussian data: the Gaussian graphical interaction model (GGIM) and the Gaussian graphical conditional expectation model (GGCEM). The development of these models comes from considering stationary Gaussian processes on graphs, and leveraging the equations between the resulting steady-state covariance matrix and the Laplacian matrix representing the interaction graph. Through the presentation of conceptually straightforward theory, we develop the new models and provide interpretations of the edges in each graphical model in terms of statistical measures. We show that when restricted to undirected graphs, the Laplacian matrix representing a GGIM is equivalent to the standard inverse covariance matrix that encodes conditional dependence relationships. We demonstrate that the problem of learning sparse GGIMs and GGCEMs for a given observation set can be framed as a LASSO problem. By comparison with the problem of inverse covariance estimation, we prove a bound on the difference between the covariance matrix corresponding to a sparse GGIM and the covariance matrix corresponding to the  $l_1$ -norm penalized maximum log-likelihood estimate. In all, the new models present a novel perspective on directed relationships between variables and significantly expand on the state of the art in Gaussian graphical modeling.

## 1. Introduction

Classically, a Gaussian graphical model (GGM) of an observation set is a graph that encodes conditional independence relationships between variables, where each variable is a node in the graph (Whittaker, 2009). That is, the presence of an edge between nodes  $i$  and  $j$  indicates that variables  $i$  and  $j$  are conditionally dependent given the remaining variables. Consequently, the absence of an edge indicates conditional independence between  $i$  and  $j$ . It is well known that the sparsity pattern of the off-diagonal elements of the precision matrix (inverse covariance matrix) encodes these conditional independence relationships.

Learning the structure of the conditional independence graph is accomplished by finding the precision matrix that balances sparsity, often with respect to the  $l_1$ -norm, with maximizing the Gaussian log-likelihood function associated with the set of i.i.d. observations (Friedman et al., 2008; Banerjee et al., 2008). The non-zero off-diagonal entries of the resulting precision matrix are then taken to be edges in the underlying conditional independence graph. As the covariance matrix is by definition symmetric, its inverse is also symmetric and therefore this approach is limited to producing only undirected graphs. The precision matrix is in fact a Laplacian matrix for an undirected graph, and the conditional independence graph can also be viewed as an undirected graph of interactions between variables.

---

\*Katherine Fitch is with the Chair of Operations Research, Technical University of Munich, Munich, Germany. [katie.fitch@tum.de](mailto:katie.fitch@tum.de)

The problem of estimating inverse covariance matrices has been extensively studied and applied to applications ranging from analysis of functional brain connectivity (Kruschwitz et al., 2015) to speech recognition (Zhang and Fung, 2013) to computer vision applications (Souly and Shah, 2016). Among estimators that regularize the Gaussian log-likelihood by the  $l_1$ -norm, there are algorithmic approaches that employ block coordinate descent (Banerjee et al., 2008), the graphical LASSO (Friedman et al., 2008), quadratic approximation (Hsieh et al., 2011), second order Newton-like methods (Oztoprak et al., 2012), and many others. Additional methods of sparsity promotion include greedy forward-backward search to determine the location of zeros in the precision matrix (Lauritzen, 1996),  $l_0$ -norm regularization (Marjanovic and Hero, 2015), and  $l_q$  penalization (Marjanovic and Solo, 2014), where  $0 \leq q < 1$ .

While GGMs and sparse inverse covariance estimation provide a straightforward and generalizable framework for approximating conditional independence relationships between variables from a sample set of observations, the question remains of how to graphically model directed interactions. For example, consider a random vector with three variables,  $a$ ,  $b$ , and  $c$ , where  $a$  influences  $b$ ,  $b$  influences  $c$ , and  $c$  influences  $a$ . The conditional independence graph would contain undirected edges between all three nodes, however, the true sparsest model of interaction would be a directed cycle from  $a$  to  $b$  to  $c$  to  $a$ . This is to say that conditional dependence between any two variables does not imply that the two variables influence each other equally, therefore, inverse covariance estimation provides limited information on the interactions between variables.

Learned directed graphical models such as Bayesian networks (Barber, 2012), and linear Gaussian structure equation models (SEMs) (Bollen, 1989) overcome some of the limitations of inverse covariance estimation by representing casual relationships between variables as edges in directed acyclic graphs (DAGs). While these models have been successfully and broadly implemented for a wide variety of applications, they still have non-trivial disadvantages. Most notably, due to their hierarchical nature, neither Bayesian networks nor SEMs can directly model cyclic interactions. As a result, the simple directed cycle from the previous paragraph cannot be accurately reproduced through these methods. This is an issue because the ability to learn and model cyclic interactions is critical to our understanding of complex systems. In a biological system, for example, cyclic interactions can be indicative of regulatory feedback loops. Thus, when attempting to learn graphical structure from data, the failure to identify feedback loops results in an incomplete understanding of the fundamental mechanisms of the biological system. There is, therefore, a need for learned graphical models of Gaussian data that represent directed relationships between variables without topological restrictions.

## 1.1 Contributions

In this paper we significantly expand the modeling capabilities for Gaussian data by exploring features that can be modeled as directed relationships, namely interactions between variables and conditional expectations of conditional independence, and developing a consistent theoretical framework uniting the model types with traditional GGMs. This theoretical framework arises from considering a sample covariance matrix to be the steady-state covariance matrix of a stationary Gaussian process on a graph. We then examine the relationship between the inverse covariance matrix and the Laplacian matrix representing the interaction graph. The subtle perspective shift to stationary Gaussian processes allows us to leverage matrix equations to a great advantage, as we are able to unite the concepts of interactions between variables and conditional dependence without the need for applying complex rules to the nodes and edges in the graph. The connection between network topology of a stationary Gaussian process and inverse covariance matrices has been previously established (for example, (Hassan-Moghaddam et al., 2016)). However, thus far

the focus has been limited to applying techniques from sparse inverse covariance estimation to the problem of *undirected* network identification.

The main contributions of this paper are the introduction of two new directed graphical models: *Gaussian graphical interaction models* (GGIMs) and *Gaussian graphical conditional expectation models* (GGCEMs). An overview of these new models and how they compare to the standard Gaussian graphical model can be found in Table 1.

Model	Edge interpretation	Edge type
GGM	conditional independence	undirected
GGIM	interaction between variables	directed & undirected
GGCEM	conditional expectation of conditional independence	directed & undirected

**Table 1:** Overview of Gaussian graphical model variants and their edge interpretations.

We demonstrate that the problem of learning  $l_1$ -norm sparse GGIMs and GGCEMs for a given observation set can be framed as a LASSO problem and provide a bound on the difference between the covariance matrix estimate corresponding to a GGIM and the maximum likelihood estimate (MLE) of the covariance matrix, as well as the  $l_1$ -norm penalized maximum log-likelihood estimate of the covariance matrix.

The GGIM and GGCEM models are mathematically elegant and intuitive, and learning sparse models is simple to implement. As the GGIM and GGCEM models are not restricted to the class of directed acyclic graphs, they are able to model a large variety of general relationships between variables that are not possible with existing graphical models. To our knowledge, this is the first paper to leverage steady-state characteristics of a stationary Gaussian process on a directed graph to develop general *directed* models from Gaussian data.

## 1.2 Example: Cell signaling network

To motivate the enhanced graphical modeling potential of GGIMs and GGCEMs, we demonstrate the two new models when applied to the same dataset as used by the authors of (Friedman et al., 2008) in their paper introducing the GLASSO algorithm for sparse precision matrix estimation. The dataset is from (Sachs et al., 2005) and contains flow cytometry data of  $n = 7466$  cells and  $p = 11$  proteins. Figure 1a reproduces the classic signaling network (Sachs et al., 2005, Figure 2).

The conditional independence graph from (Friedman et al., 2008) is shown in Figure 1b. To compare, we show the two new graph models introduced in this paper, GGIM and GGCEM, in Figures 1c and 1d, respectively. Details for computing the graphs 1c and 1d can be found in Section 5. All graphs contain 18 edges, where, in the directed setting, an edge from node  $i$  to  $j$  is counted independently from an edge  $j$  to  $i$ . Solid lines indicate edges that are present in the classic signaling graph and light gray dashed lines indicate edges that are not present in the classic signaling graph. In graphs 1c and 1d, black lines indicate edges identified in the same orientation as the classic signaling graph. Dark gray lines indicate edges identified in the reverse orientation as the classic signaling graph.

The GGIM (1c) and GGCEM (1d) graphs capture more of the edges of Figure (1a) than the undirected conditional independence graph (1b), with the majority of correctly identified edges also in the correct orientation.

**Remark 1** It is noted that GGIMs and GGCEMs inherently differ from Bayesian networks and linear Gaussian SEMs. The models in this paper arise from the steady-state characteristics of a set of equations where the *rate of change* of a variable is a linear combination of the state of

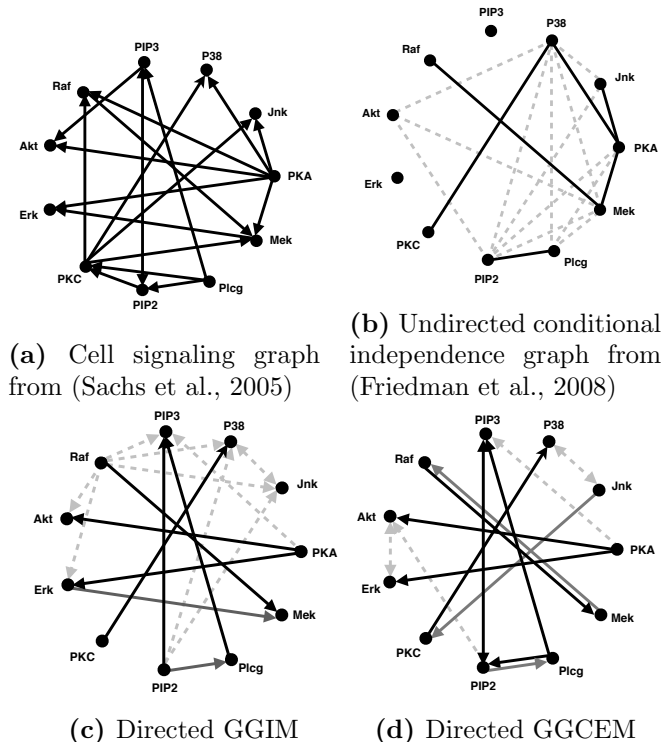


**Figure 1:** Comparison of graphical models from cell interaction data. (a). Classic signaling graph from (Sachs et al., 2005). (b). Conditional independence graph generated by the GLASSO algorithm (Friedman et al., 2008). (c). Directed GGIM. (d). Directed GGCEM. Solid lines indicate edges that are present in the classic signaling graph. Dashed light gray lines indicate edges that are not present in the classic signaling graph. In graphs (c) and (d), black lines indicate edges identified in the same orientation as the classic signaling graph. Dark gray lines indicate edges identified in the reverse orientation as the classic signaling graph.

the remaining variables. SEMs arise from a set of equations where the *state* of a variable is a linear combination of the state of parent variables. Bayesian networks and SEMs model strictly hierarchical relationships through directed edges that represent causality, whereas GGIMs and GGCEMs model the interactions between variables and conditional expectations of conditional dependence. The hierarchical nature of Bayesian networks and SEMs mandates that they are represented by DAGs, while no such restriction is placed on GGIMs or GGCEMs, which can have any general graph structure. Due to these conceptual differences we do not seek to apply notions such as Markov equivalence (Chickering, 2002), morality (Lauritzen and Spiegelhalter, 1988), or faithfulness (Zhang and Spirtes, 2003) to GGIMs or GGCEMs.

### 1.3 Outline

The remainder of the paper is organized as follows. Background and notation are provided in Section 2. In Section 3 we develop relevant theory and introduce the Gaussian Graphical Interaction Model. In Section 4 we prove a relationship between the conditional distribution of two variables and the conditional expectation of conditional independence, and introduce the Gaussian Graphical Conditional Expectation Model. Section 5 demonstrates how learning GGIMs and GGCEMs can be framed as LASSO problems and provides a bound on the estimated covariance matrix relative to the MLE of the covariance matrix for the GGIM. In Section 6 we demonstrate the performance

of a hybrid GGIM and GGCEM learning approach on the data from a former DREAM sub-challenge (Hill et al., 2016) where participants were tasked with inferring a directed network of phosphoproteins. We conclude with final remarks in Section 7.

## 2. Background and notation

Let  $\mathcal{G} = (\mathcal{V}, \mathcal{E}, A)$  be a connected, directed graph representing interactions between variables, where  $\mathcal{V} = \{1, 2, \dots, p\}$  is the set of variables (also referred to as nodes), and  $\mathcal{E} \subseteq \mathcal{V} \times \mathcal{V}$  is the set of  $m$  edges.  $A \in \mathbb{R}^{p \times p}$  is the adjacency matrix where element  $a_{i,j}$  is the weight on edge  $(i, j)$ . If  $(i, j) \in \mathcal{E}$  then  $a_{i,j} > 0$ ; otherwise  $a_{i,j} = 0$ . The *out-degree* of node  $i$  is calculated as  $d_i = \sum_{j=1}^n a_{i,j}$ . The out-degree matrix is a diagonal matrix of node out-degrees,  $D = \text{diag}\{d_1, d_2, \dots, d_p\}$ . The associated directed *Laplacian* matrix is defined as  $L = D - A$ . This corresponds to a ‘sensing’ interpretation of node interactions where an edge from  $i$  to  $j$  indicates that node  $i$  senses the state of node  $j$ . We primarily consider this interpretation of edge orientation to maintain consistency with previous research on Gaussian processes on directed graphs, e.g. (Fitch, 2019; Young et al., 2016). The transposed Laplacian corresponds to the ‘sending’ interpretation where an edge from  $i$  to  $j$  indicates that the state of node  $i$  is available to node  $j$ .

Throughout the paper, partitioning of a given matrix,  $G$ , will follow

$$G = \begin{bmatrix} G_{a,a} & G_{a,b} \\ G_{a,b}^T & G_{b,b} \end{bmatrix}, \quad (1)$$

where  $G_{a,a} \in \mathbb{R}^{2 \times 2}$ .

The expected value of a random vector  $Y_a$  conditional on the random vector  $Y_b$  with mean and covariance given by:

$$\begin{bmatrix} Y_a \\ Y_b \end{bmatrix} \sim \mathcal{N} \left( \begin{bmatrix} \nu_a \\ \nu_b \end{bmatrix}, \begin{bmatrix} \Sigma_{a,a} & \Sigma_{a,b} \\ \Sigma_{b,a} & \Sigma_{b,b} \end{bmatrix} \right), \quad (2)$$

is

$$\mathbb{E}(Y_a|Y_b) = \nu_{Y_a|Y_b} = \nu_a + \Sigma_{a,b}(\Sigma_{b,b})^{-1}(Y_b - \nu_b), \quad (3)$$

with conditional distribution

$$\Sigma_{a|b} = \Sigma_{a,a} - \Sigma_{a,b}(\Sigma_{b,b})^{-1}\Sigma_{a,b}^T.$$

The sample mean of  $n$  independent and identically distributed (i.i.d.) observations  $X^{(1)}, \dots, X^{(n)}$  from  $\mathcal{N}(\mu, \Sigma)$ , is

$$\bar{X} = \frac{1}{n} \sum_{i=1}^n X^{(i)}.$$

The sample covariance matrix is

$$S = \frac{1}{n} \sum_{i=1}^n (X^{(i)} - \bar{X})(X^{(i)} - \bar{X})^T,$$

and is equal to the Maximum Likelihood Estimate (MLE) of the covariance matrix.

In Sections 3 and 4 the Laplacian matrix, covariance matrix, and sample covariance matrix are all assumed to be full rank and corresponding to a weakly connected graph. The limiting case of

GGIMs associated with a positive semi-definite covariance matrix is considered in Appendix A. In Section 5 we assume that the number of observations,  $n$ , is greater than the number of variables,  $p$ . However, we note that the corresponding LASSO problems can nevertheless be solved in the case  $n \leq p$ .

The  $l_1$ - norm of a matrix is defined as the sum of absolute values of elements in the matrix and the  $l_\infty$ -norm of a matrix is defined as the maximum absolute value of elements in the matrix. Recall that a skew-symmetric matrix,  $\kappa$ , satisfies  $\kappa^T = -\kappa$ . We denote the set of all  $\mathbb{R}^{p \times p}$  skew-symmetric matrices by  $\text{so}(p)$ .

### 3. Gaussian graphical interaction models

We begin this section by reviewing the relationship between conditional independence and the inverse covariance matrix for a random vector  $X$  with Gaussian distribution  $\mathcal{N}(0, \Sigma)$ . Then, we provide a lemma relating the inverse covariance matrix of  $X$  to the undirected interaction graph for a stationary Gaussian process  $\mathbf{x}$  with distribution  $\mathcal{N}(0, \Sigma)$ . Next, we discuss how the Gaussian process viewpoint allows us to consider directed interactions between variables. The section concludes with the definition for a new directed graphical model, the Gaussian graphical interaction model.

There are multiple approaches for demonstrating that the sparsity pattern of the precision matrix is representative of the underlying undirected independence graph structure. For example, by using Schur complements it is possible to show that zeros in the precision matrix correspond to conditional independence relationships (Anderson, 2003). Consider a covariance matrix partitioned as in (1), where  $\Sigma_{a,a} \in \mathbb{R}^{2 \times 2}$  contains elements indexed by 1, 2, and let  $P = \Sigma^{-1}$ . Then, the submatrix  $P_{a,a}$  can be written as

$$P_{a,a} = (\Sigma_{a,a} - \Sigma_{a,b}(\Sigma_{b,b})^{-1}\Sigma_{a,b}^T)^{-1}.$$

Therefore  $P_{a,a}$  is the inverse of the conditional covariance,  $\Sigma_{a|b}$ , and two-by-two matrix inversion,  $P_{1,2} = 0$  implies that  $\Sigma_{1,2|b} = 0$ . In other words, variables indexed by  $i$  and  $j$  are conditionally independent given the remaining variables if and only if  $P_{i,j} = \Sigma_{i,j}^{-1} = 0$ .

We now demonstrate that the same relationship between the precision matrix and the underlying graph can be established from dynamic systems perspective. Rather than think of the  $n$  i.i.d. samples as drawn from a multivariate normal distribution, they can be thought of as belonging to a stationary Gaussian process. Recall, for a stochastic process to be stationary its unconditional joint probability distribution is unchanged under time shifts. This further implies that the mean and covariance do not change over time. Before stating the lemma regarding the relationship between inverse covariance matrix of a random vector and the interaction graphs of stationary Gaussian processes, we first provide a theorem from (Arnold, 1992). In the following,  $d\mathbf{W}$  represents increments drawn from independent Wiener processes.

**Theorem 2** (From (Arnold, 1992)) *The solution of the equation*

$$d\mathbf{x} = (M(t) + a(t))\mathbf{x}dt + B(t)d\mathbf{W}, \quad \mathbf{x}_{t_0} = c, \quad (4)$$

*is a stationary Gaussian process if  $M(t) \equiv M$ ,  $a(t) \equiv 0$ ,  $B(t) \equiv B$ , the eigenvalues of  $M$  have negative real parts, and  $c$  is  $\mathcal{R}(0, K)$ -distributed, where  $\Sigma$ , the steady-state covariance matrix, is*

$$\Sigma = \int_0^\infty e^{Mt} B B^T e^{M^T t} dt,$$

*or equivalently the solution of the Lyapunov equation*

$$M\Sigma + \Sigma M^T = -B B^T.$$

**Lemma 3** Consider a stationary Gaussian process  $\mathbf{x} \in \mathbb{R}^p$  with multivariate Gaussian distribution  $\mathcal{N}(0, \Sigma)$  and a random vector  $X \in \mathbb{R}^p$  with multivariate Gaussian distribution  $\mathcal{N}(0, \Sigma)$ . Then, up to a scaling, the unique symmetric Laplacian matrix corresponding to the steady-state undirected interaction graph associated with  $\mathbf{x}$  is equal to the inverse covariance matrix associated with the random vector  $X$ .

**Proof**

Consider equation (4) in the context of a stochastic process on a graph by replacing  $M$  with the negative graph Laplacian  $-L$  and taking  $B = \sigma I_p$ . The resulting equation,

$$d\mathbf{x} = -L\mathbf{x}dt + \sigma d\mathbf{W}, \tag{5}$$

represents a noisy diffusion process where each node  $i$  in the graph averages its state,  $\mathbf{x}_i$ , with the state of its neighbors, subject to noise in the state of each node with standard deviation  $\sigma$ . Without loss of generality, let  $\sigma^2 = 2$ . As the eigenvalues of  $-L$  have negative real parts, the solution  $\mathbf{x}$  is a stationary process. The corresponding steady-state covariance matrix is the unique solution to

$$L\Sigma + \Sigma L^T = 2I_p. \tag{6}$$

When restricting to only undirected graphs ( $L$  symmetric), the unique solution  $\Sigma = L^{-1}$  satisfies (6). ■

Therefore, we have demonstrated that for undirected graphical models, the stationary Gaussian diffusion process represented by the steady-state dynamics of  $\mathbf{x}$  recovers the relationship between the precision matrix and graph structure, up to a scaling. More specifically, by the relationship  $L = \Sigma^{-1}$ , the non-zero elements of the inverse covariance matrix indicate both conditional dependencies and edges in the underlying interaction graph.

Returning to the stationary Gaussian process (5), we can ask what happens when  $L$  represents a directed graph and is no longer symmetric. In this case, the solution  $\Sigma$  to (6) still exists, is unique, and is symmetric, but is no longer a scale of the inverse Laplacian matrix. In the reverse direction, given a covariance matrix,  $\Sigma$ , a corresponding  $L$  is not unique. We formalize the relationship between a  $L$  and  $\Sigma$  in the following proposition, which follows from considering the relationships provided for rank deficient matrices in (Fitch, 2019) in the context of full-rank  $L$  and  $\Sigma$ .

**Proposition 4** Consider a stationary Gaussian process  $\mathbf{x} \in \mathbb{R}^p$  with multivariate Gaussian distribution  $\mathcal{N}(0, \Sigma)$ . Then the Laplacian matrices corresponding to the family of steady-state equivalent interaction graphs between the  $p$  variables of  $\mathbf{x}$  are given as a function of  $\kappa \in \mathbb{R}^{p \times p}$  skew-symmetric matrices, by

$$L(\kappa) = (I_p + \kappa)\Sigma^{-1}. \tag{7}$$

**Proof** Direct substitution yields

$$L\Sigma + \Sigma L^T = (I_p + \kappa)\Sigma^{-1}\Sigma + \Sigma\Sigma^{-1}(I_p - \kappa) = I_p + \kappa + I_p - \kappa = 2I_p.$$

It can be shown (i.e. (Barnett and Storey, 1967)) that there do not exist any Laplacian matrices corresponding steady-state equivalent interaction graphs outside of those that can be decomposed as (7). ■

This leads to the definition of the Gaussian Graphical Interaction Model:

**Definition 5 (Gaussian Graphical Interaction Model (GGIM))** Consider a stationary Gaussian process with multivariate distribution  $\mathcal{N}(0, \Sigma)$ . Then a Gaussian Graphical Interaction Model for the stationary process is the graph induced by the Laplacian matrix  $\hat{L}$  where

$$\begin{aligned}\hat{L} &= (I_p + \kappa)\Sigma^{-1}, \\ \kappa &= \arg \min_{\tilde{\kappa} \in so(p)} \|(I + \tilde{\kappa})\Sigma^{-1}\|_q,\end{aligned}$$

for a matrix norm  $0 \leq q \leq \infty$ .

**Remark 6** While constructing a directed interaction model based on a symmetric covariance matrix may seem at first counter intuitive, we note that for the  $l_1$ -norm, finding the sparsest directed matrix  $L$  that satisfies (6) inherently provides a generalization of a very natural assumption on edge directions. To illustrate, consider a two variable example consistent with the sending interpretation of variable interaction (corresponding to  $L^T$ ). If  $\Sigma_{1,1} > \Sigma_{2,2}$  then the resulting  $l_1$ -norm sparsest GGIM will contain an edge from 2 to 1. In a sense, this assumes the variable with less uncertainty passes information to the variable with higher uncertainty. The directed edge in this example represents the sparsest interaction that could lead to the covariance matrix  $\Sigma$ .

#### 4. Gaussian graphical conditional expectation models

In this section, we show that the matrix equation (6) defines pairwise relationships between the conditional expectations of two random vectors related to variables  $j, k$ , and the conditional distribution of  $j$  and  $k$  given the remaining variables. We begin by stating a theorem defining the relationship and then enter a discussion on the implications of the theorem and how it can be interpreted in the context of conditional expectations of conditional dependencies between variables.

**Theorem 7** Consider a stationary Gaussian process  $\mathbf{x} \in \mathbb{R}^p$  with multivariate distribution  $\mathcal{N}(0, \Sigma)$  and Laplacian matrix  $L$  for which (6) is satisfied. Consider  $p$  random vectors  $\begin{bmatrix} Y_{a,i} \\ Y_{b,i} \end{bmatrix}$ ,  $i = 1, \dots, p$ , distributed according to

$$\begin{bmatrix} Y_{a,i} \\ Y_{b,i} \end{bmatrix} \sim N\left(\begin{bmatrix} L_{a,i} \\ L_{b,i} \end{bmatrix}, \begin{bmatrix} \Sigma_{a,a} & \Sigma_{a,b} \\ \Sigma_{b,a} & \Sigma_{b,b} \end{bmatrix}\right).$$

Then for any pair  $j \neq k$ , with  $c = \mathcal{V} \setminus \{j, k\}$ , the following holds

$$\mathbb{E}(Y_{j,k}|P_{c,k})\left(\frac{(\Sigma_{j,k|c})^2 - \Sigma_{k|c}}{\Sigma_{j|c}}\right) + \mathbb{E}(Y_{k,j}|P_{c,j})\left(\frac{(\Sigma_{j,k|c})^2}{\Sigma_{k|c}} - \Sigma_{j|c}\right) = \frac{\Sigma_{j,k|c}}{\Sigma_{j|c}} + \frac{\Sigma_{j,k|c}}{\Sigma_{k|c}}. \quad (8)$$

**Proof** We begin by rewriting equation (6) as

$$\Sigma^{-1}L + L^T\Sigma^{-1} = 2(\Sigma^{-1})^2. \quad (9)$$

Let  $\Sigma$  and  $L$  be partitioned according to (1), where  $\Sigma_{a,a}$ ,  $L_{a,a} \in \mathbb{R}^{2 \times 2}$  are indexed by 1, 2, and express  $\Sigma^{-1}$  as

$$\Sigma^{-1} = P = \begin{bmatrix} (\Sigma_{a|b})^{-1} & -(\Sigma_{a|b})^{-1}\Sigma_{ab}(\Sigma_{b,b})^{-1} \\ -(\Sigma_{b,b})^{-1}\Sigma_{ab}(\Sigma_{a|b})^{-1} & (\Sigma_{b,b})^{-1} + (\Sigma_{b,b})^{-1}\Sigma_{ab}(\Sigma_{a|b})^{-1}\Sigma_{ab}(\Sigma_{b,b})^{-1} \end{bmatrix}.$$



Then, the top left submatrix of (9) can be expanded as

$$\begin{aligned} & (\Sigma_{a|b})^{-1}L_{a,a} - (\Sigma_{a|b})^{-1}\Sigma_{a,b}(\Sigma_{b,b})^{-1}L_{b,a} + L_{a,a}^T(\Sigma_{a|b})^{-1} - L_{a,b}^T(\Sigma_{b,b})^{-1}\Sigma_{a,b}(\Sigma_{a|b})^{-1} \\ & = 2(\Sigma_{a|b})^{-2} + 2(\Sigma_{a|b})^{-1}\Sigma_{a,b}(\Sigma_{b,b})^{-1}(\Sigma_{b,b})^{-1}\Sigma_{a,b}(\Sigma_{a|b})^{-1}. \end{aligned}$$

Multiplying both sides by  $\Sigma_{a|b}$  yields

$$(L_{a,a} - \Sigma_{a,b}(\Sigma_{b,b})^{-1}L_{b,a})\Sigma_{a|b} + \Sigma_{a|b}(L_{a,a}^T - L_{a,b}^T(\Sigma_{b,b})^{-1}\Sigma_{a,b}) = 2I + 2\Sigma_{a,b}(\Sigma_{b,b})^{-1}(\Sigma_{b,b})^{-1}\Sigma_{a,b}.$$

Substituting  $P_{a,b} = -(\Sigma_{a|b})^{-1}\Sigma_{ab}(\Sigma_{b,b})^{-1}$  and rearranging gives

$$\left( L_{a,a} + \Sigma_{a,b}(\Sigma_{b,b})^{-1}(P_{b,a} - L_{b,a}) \right) \Sigma_{a|b} + \Sigma_{a|b} \left( L_{a,a} + \Sigma_{a,b}(\Sigma_{b,b})^{-1}(P_{b,a} - L_{b,a}) \right)^T = 2I. \quad (10)$$

Recalling (2) and (3), the terms of (10) in parenthesis can be interpreted as the expected values of the precision submatrix conditioned on entries from the corresponding columns  $P_{b,1}$ ,  $P_{b,2}$ . This is seen by considering random vectors with mean values as the first and second columns of the Laplacian matrix, respectively, and covariance matrix  $\Sigma$ , i.e.,

$$\begin{bmatrix} Y_{a,1} \\ Y_{b,1} \end{bmatrix} \sim N \left( \begin{bmatrix} L_{a,1} \\ L_{b,1} \end{bmatrix}, \begin{bmatrix} \Sigma_{a,a} & \Sigma_{a,b} \\ \Sigma_{b,a} & \Sigma_{b,b} \end{bmatrix} \right), \quad \begin{bmatrix} Y_{a,2} \\ Y_{b,2} \end{bmatrix} \sim N \left( \begin{bmatrix} L_{a,2} \\ L_{b,2} \end{bmatrix}, \begin{bmatrix} \Sigma_{a,a} & \Sigma_{a,b} \\ \Sigma_{b,a} & \Sigma_{b,b} \end{bmatrix} \right).$$

That is,

$$\begin{aligned} \tilde{P}_{a,1} &= \mathbb{E}(Y_{a,1}|P_{b,1}) = L_{a,1} + \Sigma_{a,b}(\Sigma_{b,b})^{-1}(P_{b,1} - L_{b,1}), \\ \tilde{P}_{a,2} &= \mathbb{E}(Y_{a,2}|P_{b,2}) = L_{a,2} + \Sigma_{a,b}(\Sigma_{b,b})^{-1}(P_{b,2} - L_{b,2}), \end{aligned}$$

and

$$\tilde{P}_{a,a}\Sigma_{a|b} + \Sigma_{a|b}\tilde{P}_{a,a}^T = 2I. \quad (11)$$

The off-diagonal components of the matrix equation (11) give

$$\left( \mathbb{E}(Y_{1,1}|P_{b,1}) + \mathbb{E}(Y_{2,2}|P_{b,2}) \right) \Sigma_{1,2|b} + \mathbb{E}(Y_{1,2}|P_{b,2})\Sigma_{2|b} + \mathbb{E}(Y_{2,1}|P_{b,1})\Sigma_{1|b} = 0. \quad (12)$$

The terms  $\mathbb{E}(Y_{1,1}|P_{b,1})$  and  $\mathbb{E}(Y_{2,2}|P_{b,2})$  can be solved for from the diagonal elements of (11) and substituted in to (12). As the resulting relationship must hold pairwise for any two nodes, we have that for any  $j, k$ , where  $j \neq k$  and the set of nodes excluding  $j, k$ ,  $c = \mathcal{V} \setminus \{j, k\}$ ,

$$\mathbb{E}(Y_{j,k}|P_{c,k}) \left( \frac{(\Sigma_{j,k|c})^2 - \Sigma_{k|c}}{\Sigma_{j|c}} \right) + \mathbb{E}(Y_{k,j}|P_{c,j}) \left( \frac{(\Sigma_{j,k|c})^2}{\Sigma_{k|c}} - \Sigma_{j|c} \right) = \frac{\Sigma_{j,k|c}}{\Sigma_{j|c}} + \frac{\Sigma_{j,k|c}}{\Sigma_{k|c}}. \quad \blacksquare$$

Equations (8), and (11) provide new interpretations and insights on graphical modeling. First, a column,  $i$ , of a Laplacian matrix,  $L$ , that satisfies (6) for a given  $\Sigma$  can be thought of expected values for incoming edges to node  $i$ . Second, using  $\Sigma$  and the expected values for incoming edges, we can calculate the expected value of entries in a precision submatrix of nodes  $i$ , and  $j$  conditioned on the remainder of the  $i$ -th and  $j$ -th columns of the precision matrix.

Due to the relationship between the precision matrix and conditional covariances, the conditional expectations of the precision matrix answers two questions: first given the conditional dependencies of  $i$  with all nodes except  $j$ , and the expected values of all edges incoming to  $i$ , is it

expected that  $i$  and  $j$  are conditionally independent? Second, given the conditional dependencies of  $j$  with all nodes except  $i$ , and the expected values of all edges incoming to  $j$ , is it expected that  $i$  and  $j$  are conditionally independent? Clearly, if the underlying interaction graph is directed, the answers to these two questions are not necessarily equivalent.

Equation (8) represents a balance equation between pairs of variables. Consider the case where  $\Sigma_{j|b} = \Sigma_{k|b}$ , and  $j$  and  $k$  are conditionally independent ( $\Sigma_{j,k|b} = 0$ ). Then (8) reduces to

$$\mathbb{E}(Y_{k,j}|P_{b,k}) = -\mathbb{E}(Y_{j,k}|P_{b,j}).$$

In other words, the conditional expectation of an edge from  $k$  to  $j$  in the conditional independence graph is canceled out by an equal magnitude negative conditional expectation of an edge from  $j$  to  $k$ .

We leverage the interpretation of the relationship (8) to define Gaussian Graphical Conditional Expectation Models as follows:

**Definition 8 (Gaussian Graphical Conditional Expectation Model (GGCEM))** Consider a stationary Gaussian process with multivariate distribution  $\mathcal{N}(0, \Sigma)$ . Then a Gaussian Graphical Conditional Expectation Model for the stationary process is the graph induced by the Adjacency matrix  $\hat{P}$  where

$$\hat{P} = \arg \min_{\tilde{P}} \|\tilde{P}\|_q,$$

such that

$$\tilde{P}_{j,k} \left( \Sigma_{k|c} - \frac{(\Sigma_{j,k|c})^2}{\Sigma_{j|c}} \right) + \tilde{P}_{k,j} \left( \Sigma_{j|c} - \frac{(\Sigma_{j,k|c})^2}{\Sigma_{k|c}} \right) = \frac{\Sigma_{j,k|c}}{\Sigma_{j|c}} + \frac{\Sigma_{j,k|c}}{\Sigma_{k|c}} \quad \forall j \neq k; c = \{\mathcal{V} \setminus \{j, k\}\}, \quad (14)$$

for a matrix norm  $0 \leq q \leq \infty$ .

## 5. Learning sparse GGIMs and GGCEMs

Typically the true covariance matrix,  $\Sigma$  of a Gaussian process is unknown, and therefore the graphical models must be estimated from a set of observations. Informally, the optimization problems associated with learning GGIMs and GGCEMs are stated as: Given observations from a stationary Gaussian process, jointly estimate  $\hat{\Sigma}$  and  $\hat{L}$  ( $\hat{P}$ ) that yield the sparsest directed GGIM (GGCEM) while sufficiently fitting the sample data. In the following section we formulate the GGIM and GGCEM learning problems mathematically and provide a bound on the covariance matrix estimate in the case of GGIM learning.

To emphasize the theoretical continuity between GGIMs, GGCEMs, and inverse covariance matrices, we adopt the  $l_1$ -norm sparsity objective that is often included in inverse covariance estimation. Naturally, there is no guarantee that the  $l_1$ -norm is truly the best penalization for all real world data sets. One could consider learning GGIMs and GGCEMs with other sparsity promoting terms, however, this is outside the scope of this work.

### 5.1 Sparse GGIM learning

Consider  $n$  observations  $\mathbf{x}^{(1)}, \dots, \mathbf{x}^{(n)}$  with sample covariance  $S$  from a stationary Gaussian process with multivariate distribution  $\mathcal{N}(0, \Sigma)$ . A GGIM estimate without any constraints on sparsity is a graph with Laplacian matrix  $L$  for which (6) is satisfied with the maximum likelihood estimate (MLE) of the covariance matrix,  $S$ . That is,

$$LS + SL^T = 2I. \quad (15)$$

Equation (15) can be written in the form  $H\mathbf{z} = \mathbf{f}$ , where  $\mathbf{z} = \text{vec}(L)$ ,  $\mathbf{f} = \text{vec}(2I)$  and  $H \in \mathbb{R}^{1/2(p^2+p) \times p^2}$ .

A sparse GGIM estimate is a graph induced by the the solution vector  $\hat{\mathbf{z}}$  which minimizes a norm on the error term  $\mathbf{f} - H\hat{\mathbf{z}}$ , subject to sparsity penalization. Here, we consider the squared  $l_2$ -norm on the error and a sparsity penalization by way of the  $l_1$ -norm on  $\hat{\mathbf{z}}$ . This leads to the LASSO problem

$$\hat{\mathbf{z}} = \min_{\mathbf{z}} \|\mathbf{f} - H\mathbf{z}\|_2^2 + \rho\|\mathbf{z}\|_1, \quad (16)$$

where  $\rho \geq 0$ . The problem (16) can be solved with standard algorithms such as coordinate descent (Wu and Lange, 2008). We omit a discussion on LASSO problems here and refer instead to (Hastie et al., 2015) for an in-depth review of LASSO solution approaches, interpretations, and generalizations.

The associated Laplacian matrix estimate  $\hat{L}$  is the reshaped vector  $\hat{\mathbf{z}}$  such that  $\hat{L} \in \mathbb{R}^{p \times p}$ . Then, the sparse GGIM estimate is the graph induced by Laplacian matrix  $\hat{L}$ . Note that we have suppressed dependence on  $\kappa$  relative to Definition 5 because the problem of estimating  $\hat{\kappa}$  and  $\hat{\Sigma}$  such that  $\hat{L}$  is sparse and (15) approximately holds is a more difficult problem than estimating  $\hat{L}$  directly. However, for an estimate  $\hat{L}$  obtained by the solution to (16), there exists a unique  $\hat{\Sigma}$  and  $\hat{\kappa}$  that can be calculated by solving  $\hat{L}\hat{\Sigma} + \hat{\Sigma}\hat{L}^T = 2I$  and  $\hat{\kappa} = \hat{L}\hat{\Sigma} - I$ .  $\hat{L}$  as defined above is consistent with the sensing interpretation of node interaction, the more conventional sending interpretation (i.e. as applied in the example in Section 1.2 and Section 6) is obtained by  $\hat{L}^T$ .

### 5.1.1 SPARSE GGIM LEARNING WITH BOUNDED COVARIANCE

In (Friedman et al., 2008; Banerjee et al., 2008), the authors demonstrate that covariance matrix estimate that maximizes the Gaussian log-likelihood function subject to a  $l_1$  penalization on the matrix inverse is a bounded additive perturbation to the unconstrained Gaussian MLE of the covariance,  $S$ . Here, we show that in the directed GGIM learning variant, the problem can be reformulated and solved such that the additive difference between  $S$  and the estimated covariance matrix,  $\hat{\Sigma}$ , corresponding to a GGIM is bounded relative to the error on (15). This, in turn provides us with a bound on the difference between the penalized maximum likelihood estimates of (Friedman et al., 2008; Banerjee et al., 2008) and the covariance estimate corresponding to a sparse GGIM.

From (6) we have that in the unconstrained case without any penalty on the sparsity of  $L$ , the diagonal elements of  $L$  satisfy

$$L_{i,i} = \frac{1}{S_{i,i}} \left( 1 - \sum_{j \neq i} L_{i,j} S_{i,j} \right). \quad (17)$$

Substituting (17) into the equations for off-diagonal elements gives for every pair  $j \neq k$ ,

$$\sum_{i \neq j} L_{j,i} \left( \frac{S_{j,k} S_{j,i}}{S_{j,j}} - S_{k,i} \right) + \sum_{l \neq k} L_{k,l} \left( \frac{S_{j,k} S_{k,l}}{S_{k,k}} - S_{j,l} \right) = \frac{S_{j,k}}{S_{j,j}} + \frac{S_{j,k}}{S_{k,k}}. \quad (18)$$

Let  $\zeta \in \mathbb{R}^{(p^2-p) \times 1}$  be the vector of off-diagonal elements of  $L$ . Let  $\tilde{H} \in \mathbb{R}^{(p^2-p)/2 \times (p^2-p)}$  be the matrix where the elements in each row represent corresponding of  $\zeta$  for one constraint equation (18), and let  $\beta \in \mathbb{R}^{(p^2-p)/2 \times 1}$  be the vector of elements on the right side of each constraint equation (18). Then, the set of equations can be written as  $\tilde{H}\zeta = \beta$  and the corresponding LASSO problem for the off-diagonal elements of  $L$  is

$$\hat{\zeta} = \min_{\zeta} \|\beta - \tilde{H}\zeta\|_2^2 + \rho\|\zeta\|_1. \quad (19)$$

Let  $\hat{L}$  be such that the off-diagonal elements are the appropriate components of the reshaped vector  $\hat{\zeta}$  and the diagonal elements satisfy

$$\hat{L}_{i,i} = \frac{1}{S_{i,i}} \left( 1 - \sum_{l \neq i} \hat{L}_{i,l} S_{i,l} \right) + \epsilon_i, \quad (20)$$

where  $\epsilon_i$  is chosen such that  $L^{(k)} = (I \otimes \hat{L} + \hat{L}^T \otimes I)$  is strictly diagonally dominant. Note that it if  $\nu_r = \max_j \sum_{i \neq j} |\hat{L}_{j,i}|$  and  $\nu_c = \max_j \sum_{i \neq j} |\hat{L}_{i,j}|$ , it suffices to set  $\epsilon_i$  such that  $L_{i,i} > \nu_r + \nu_c, \forall i$ .

Before stating the theorem bounding the covariance matrix estimate  $\hat{\Sigma}$  corresponding to the GGIM estimate  $\hat{L}$ , we first state a Lemma from (Varga, 1976).

**Lemma 9** (from (Varga, 1976)) *Assume that  $A \in \mathbb{C}^{p \times p}$  is strictly diagonally dominant and let  $\alpha = \min_i \{ |A_{i,i}| - \sum_{i \neq j} |A_{i,j}| \}$ . Then  $\|A^{-1}\|_\infty \leq \frac{1}{\alpha}$ .*

**Theorem 10** *Let  $\xi = \|\mathbf{f} - H\hat{\zeta}'\|_2$  where  $\hat{\zeta}' = \text{vec}(\hat{L})$ . Furthermore, let  $\hat{L}$  be such that  $L^{(k)}$  is strictly diagonally dominant with  $\alpha = \min_i \{ |L_{i,i}^{(k)}| - \sum_{i \neq j} |L_{i,j}^{(k)}| \}$ . Then, the covariance matrix implicitly estimated by (19) and (20),  $\hat{\Sigma}$ , satisfying  $\hat{L}\hat{\Sigma} + \hat{\Sigma}\hat{L}^T = 2I_p$  is bounded with respect to the unconstrained MLE of the covariance matrix,  $S$ , by*

$$\|\hat{\Sigma} - S\|_\infty \leq \frac{\xi}{\alpha}.$$

**Proof** Let  $\mathbf{c} = \mathbf{f} - H\hat{\zeta}'$  and let  $C$  be  $\mathbf{c}$  reshaped such that  $C \in \mathbb{R}^{p \times p}$ . Then,

$$\hat{L}S + S\hat{L}^T = 2I + C. \quad (21)$$

Combining (21) with  $\hat{L}\hat{\Sigma} + \hat{\Sigma}\hat{L}^T = 2I$  yields

$$\hat{L}(\hat{\Sigma} - S) + (\hat{\Sigma} - S)\hat{L}^T = C, \quad (22)$$

which can be written as

$$\text{vec}(\hat{\Sigma} - S) = (I \otimes \hat{L} + \hat{L}^T \otimes I)^{-1} \mathbf{c}.$$

Taking the infinity norm and applying Lemma 9 gives

$$\begin{aligned} \|\text{vec}(\hat{\Sigma} - S)\|_\infty &\leq \|(I \otimes \hat{L} + \hat{L}^T \otimes I)^{-1}\|_\infty \|\mathbf{c}\|_\infty \leq \|(I \otimes \hat{L} + \hat{L}^T \otimes I)^{-1}\|_\infty \|\mathbf{c}\|_2, \\ \|\hat{\Sigma} - S\|_\infty &\leq \frac{\xi}{\alpha}. \end{aligned}$$

■

**Corollary 11** *Let  $\tilde{\Sigma}$  be the covariance matrix estimate obtained by solving the  $l_1$ -norm penalized maximum likelihood problem  $\tilde{\Sigma} = \arg \max_{Z \succ 0} -\log \det Z - \text{trace}(SZ^{-1}) - \lambda \|Z^{-1}\|_1$ . Let  $\hat{\Sigma}$  be the covariance matrix estimate for which Theorem 10 is satisfied. Then,*

$$\|\tilde{\Sigma} - \hat{\Sigma}\|_\infty \leq \frac{\xi}{\alpha} + \lambda.$$

**Proof** From (Banerjee et al., 2008) we have that  $\tilde{\Sigma} = S + \tilde{U}$ , where  $\|\tilde{U}\|_\infty \leq \lambda$ . Plugging  $S$  in to the statement of Theorem 10 yields

$$\|\hat{\Sigma} - S\|_\infty = \|\hat{\Sigma} - \tilde{\Sigma} + \tilde{U}\|_\infty \leq \frac{\xi}{\alpha}.$$

Recall that for arbitrary  $a, b$  we have that  $\|a\| \leq \|a + b\| + \|b\|$ . Thus,

$$\|\hat{\Sigma} - \tilde{\Sigma}\|_\infty \leq \frac{\xi}{\alpha} + \lambda. \quad \blacksquare$$

We have shown, therefore, that the maximum additive difference between an estimated covariance matrix corresponding to a GGIM and the  $l_1$ -norm penalized maximum likelihood estimate of covariance is bounded.

## 5.2 Sparse GGCEM learning

Consider  $n$  observations  $\mathbf{x}^{(1)}, \dots, \mathbf{x}^{(n)}$  from a stationary Gaussian process with multivariate distribution  $\mathcal{N}(0, \Sigma)$  with sample covariance  $S$ . A GGCEM estimate without any constraints on sparsity is a graph with Adjacency matrix  $\tilde{P}$  for which (14) is satisfied with the MLE of the covariance matrix,  $S$ . That is for every  $j, k$ , and  $c = \{\mathcal{V} \setminus \{j, k\}\}$ ,

$$\tilde{P}_{j,k} \left( S_{k|c} - \frac{(S_{j,k|c})^2}{S_{j|c}} \right) + \tilde{P}_{k,j} \left( S_{j|c} - \frac{(S_{j,k|c})^2}{S_{k|c}} \right) = \frac{\Sigma_{j,k|c}}{\Sigma_{j|c}} + \frac{\Sigma_{j,k|c}}{\Sigma_{k|c}} \quad \forall j \neq k. \quad (23)$$

Equation (23) can be written in the form

$$W\mathbf{y} = \mathbf{d}, \quad (24)$$

where  $\mathbf{y} \in \mathbb{R}^{(p^2-p) \times 1}$  is the vector of off-diagonal elements of  $\tilde{P}$ ,  $\mathbf{d} \in \mathbb{R}^{(p^2-p)/2 \times 1}$  is the vector of elements on the right side of each constraint equation (23), and  $W \in \mathbb{R}^{1/2(p^2-p) \times p^2-p}$  is the matrix with rows as the coefficients of  $\tilde{P}$  for each equation (23).

A sparse GGCEM estimate is a graph induced by the the solution vector  $\hat{\mathbf{y}}$  which minimizes a norm on the error term  $W\hat{\mathbf{y}}$ , subject to sparsity penalization. Here, we again the squared  $l_2$ -norm on the error and and  $l_1$ -norm sparsity penalization on  $\hat{\mathbf{y}}$ . This leads to the LASSO problem

$$\hat{\mathbf{y}} = \min_{\mathbf{y}} \|\mathbf{d} - W\mathbf{y}\|_2^2 + \rho \|\mathbf{y}\|_1, \quad (25)$$

where  $\rho \geq 0$ .

The associated Adjacency matrix estimate  $\hat{P}$  is the matrix with off-diagonal entries filled by the vector  $\hat{\mathbf{z}}$  such that  $\hat{P} \in \mathbb{R}^{p \times p}$ . Then, the sparse GGCEM estimate is the graph induced by Adjacency matrix  $\hat{P}$ .

Similarly to the GGIM, we note that  $\hat{P}$  is consistent with the sensing interpretation of node interaction, the more conventional sending interpretation (i.e. as applied in the example in Section 1.2) is obtained by  $\hat{P}^T$ .

We note that in simulation, constructing the LASSO problem from Equation (11) frequently led to a higher percentage of correctly identified edges. This formulation corresponds to three equations for each pair  $i, j$  and subsequently a feature matrix  $\tilde{W} \in \mathbb{R}^{3/2(p^2-p) \times 2p^2}$ , where all coefficients corresponding to the diagonal components of (11) for each pair  $i, j$  are discarded after finding the LASSO solution. Due to the increased size of the feature matrix, we suggest this formulation for learning GGCEMs from observations with a relatively small number of variables, such as the in example shown in Section 1.2.

## 6. Example: HPN-DREAM breast cancer network inference sub-challenge

As a second example, we consider sub-challenge 1B from the HPN-DREAM breast cancer network inference challenge (Hill et al., 2016). For the sub-challenge, time-course data generated from a state-of-the-art dynamical model of signaling was provided with the goal of learning a directed network from the data. The training data set contained the time-courses for 20 anonymized phosphoproteins under various combinations of stimuli and inhibitions. Participants in the challenge were asked to submit a directed network with edge scores representing confidence in the presence of each edge.

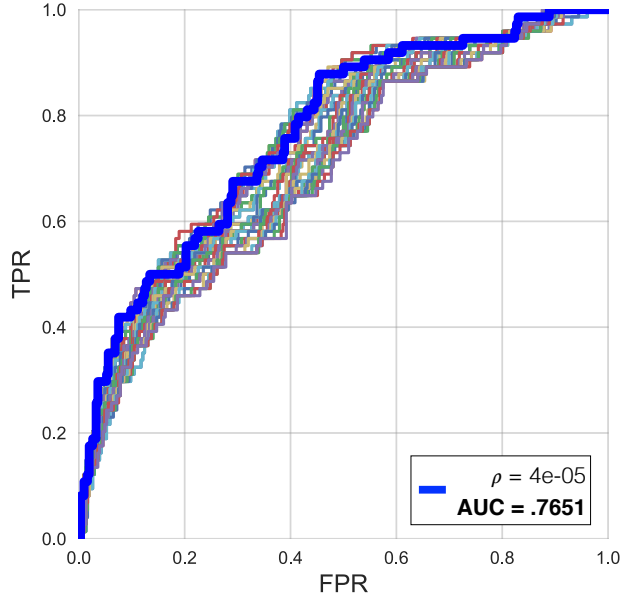
To judge the submitted networks, the edge scores were compared against a gold-standard directed network to construct a receiver operating characteristic (ROC) curve, and the area under the ROC curve (AUC) was used to determine a final ranking of all participants. An ROC curve plots the false positive rate (FPR) of a binary classifier against the true positive rate (TPR) at different discrimination thresholds. In this context, the AUC represents the probability that a uniformly drawn random true edge in the network has a higher edge score than a uniformly drawn random absent edge. An AUC of 0.5 corresponds to a model where 50% of the predictions are correct.

To test our methods on the sub-challenge data set, we grouped the time courses by combinations of stimuli and inhibitors and shifted the data of each phosphoprotein by its average value at time 0. We then set a value for  $\rho$  and solved both (16) and (25) for the data of each stimulus and inhibition pair, 20 in total, resulting in 40 graphical models. To obtain the edge scores we simply added the absolute values of the Laplacian matrices for each graphical model together, scaled by the inverse trace of the respective covariance matrices. We refer to this procedure for determining edge scores as GGIM+GGCEM. Using the edge scores and the gold-standard directed network we calculated the ROC curve and AUC associated with each value of  $\rho$ . This process was conducted for a wide range of  $\rho$ , from 0.00001 to 0.000225, which corresponds to edge densities of approximately 200 edges to 65 edges per graphical model, respectively.

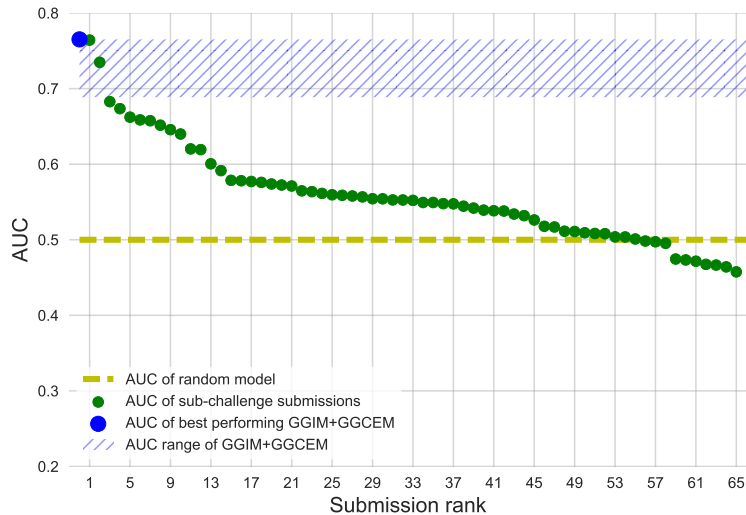
The resulting ROC curves are displayed for the range of  $\rho$  in Figure 2. The highest AUC was  $AUC = .7651$ , corresponding to  $\rho = .00004$ . The associated ROC curve is shown by a bold blue line in Figure 2.

Figure 3 shows the AUC of the 65 submissions to the sub-challenge, along with the AUC of best performing GGIM+GGCEM set of edge scores and the range of AUCs from the GGIM+GGCEM approach associated with varying  $\rho$ . It can be seen that with the correct selection of  $\rho$ , the GGIM+GGCEM approach out-performs every submission to the HPN-DREAM breast cancer network inference sub-challenge. Furthermore, even with a sub-optimal selection of  $\rho$ , our approach consistently scores among the top three submissions.

These results are extremely encouraging as they demonstrate that GGIMs and GGCEMs can provide a high level of model prediction accuracy even when the underlying processes are complex. Additionally, the results suggest that even better performance could be achieved by integrating GGIM and/or GGCEM learning with known characteristics of the underlying processes. To demonstrate the simplicity of our approach, we did not apply any biological knowledge or knowledge related to the characteristics of signaling networks. Furthermore, we made no use of the time course characteristics of the data. Appropriately accommodating these features into the calculation of edge scores has the potential to further improve predictive accuracy.



**Figure 2:** ROC curve for learned GGIM+GGCEM graphical models with  $0.00001 \leq \rho \leq 0.000225$ . ROC curve for the model with the highest AUC = .7651 is shown by the bold blue line and corresponds to  $\rho = .00004$ .



**Figure 3:** AUC of the 65 submissions to the sub-challenge (green circles), AUC of best performing GGIM+GGCEM set of edge scores (blue circle), range of AUCs from the GGIM+GGCEM approach associated with varying  $\rho$  (blue hash lines), and AUC of random model (yellow dashed line) for reference.

## 7. Final Remarks

In this paper, we have defined two new graphical models from Gaussian data, the Gaussian graphical interaction model and the Gaussian graphical conditional expectation model. To our knowledge these are the first *directed* Gaussian models with arbitrary topology. Stationary Gaussian processes

on graphs provides a theoretical basis for the models. By leveraging the Lyapunov equations between steady-state covariance matrices and the Laplacian matrices of interaction graphs, we are able to characterize families of directed graphs with equivalent steady-state behavior. A GGIM represents the sparsest graph from this family and a GGCEM represents the associated sparsest graph of conditional expectation of conditional independence. We have shown that the problem of learning GGIMs and GGCEMs can be formulated as a LASSO problem when the measure of sparsity is taken to be the  $l_1$ -norm. Moreover, we have proven that the estimated covariance matrix associated with a learned GGIM is bounded with respect to the standard  $l_1$ -norm penalized maximum log-likelihood estimate. Two examples have demonstrated that these models, though conceptually straightforward and easy to implement, perform remarkably well on real-world data and can accurately capture edge directions. In particular, the second example demonstrates that our approach has the potential to out-perform other state of the art methods. The two models open up new avenues for the modeling of directed relationships from Gaussian data and significantly expand upon the capabilities of Gaussian graphical modeling.

## Acknowledgments

This work was supported by the Alexander von Humboldt Foundation with funds from the German Federal Ministry of Education and Research (BMBF).

## A. GGIMs with positive semi-definite covariance matrices

In this section we discuss GGIMs when the sample covariance matrix is positive semi-definite. In this case we borrow from (Fitch, 2019) and apply simple projections to accommodate the rank deficiency of the sample covariance matrix. We begin by reviewing some definitions from (Fitch, 2019).

Let  $\mathbf{e}_n^{(k)}$  be the  $k$ th standard basis vector for  $\mathbb{R}^n$ . Let  $P_n = I_n - \frac{1}{n}\mathbf{1}_n\mathbf{1}_n^T$ . Let  $\mathbf{1}_n^\perp = \text{span}\{\mathbf{1}_n\}^\perp$  be the subspace of  $\mathbb{R}^n$  perpendicular to  $\mathbf{1}_n$ . Let  $Q \in \mathbb{R}^{(n-1) \times n}$  be a matrix with rows that form an orthonormal basis for  $\mathbf{1}_n^\perp$ . Then the following properties hold,

$$Q\mathbf{1}_n = \mathbf{0}, \quad QQ^T = I_{n-1}, \quad Q^TQ = P_n. \quad (26)$$

The *reduced Laplacian* matrix is defined as  $\bar{L} = QLQ^T$ , and characterizes the Laplacian matrix on  $\mathbf{1}_n^\perp$ .  $\bar{L}$  has the same eigenvalues as  $L$  except for the 0 eigenvalue and is therefore invertible if the graph is connected (Young et al., 2010). We say that a graph is connected if there exists at least one globally reachable node,  $k$ . In other words, there is a directed path from every node  $i$  to  $k$ .

Let  $\Psi \in \mathbb{R}^{n \times n}$  be a projection matrix onto  $\mathbf{1}_n^\perp$ , where  $\Psi$  is not necessarily an orthogonal projection matrix and  $\Psi L = L$ , that is the image of  $L$  is contained in the kernel of  $(\Psi - I_n)$ . The intuition behind the matrix  $\Psi$  is that it characterizes the set of globally reachable nodes.

Due to the rank deficiency of  $\Sigma$ , we consider the Lyapunov equation (6) restricted to  $\mathbf{1}_n^\perp$ . That is, we are looking for the family of reduced Laplacian matrices,  $\bar{L}$  for which the solution,  $\bar{\Sigma}$  to  $\bar{L}\bar{\Sigma} + \bar{\Sigma}\bar{L}^T = 2I_{p-1}$ , is  $\bar{\Sigma} = Q\Sigma Q^T$ . The following proposition follows from statements in (Fitch, 2019).

**Proposition 12** *Consider a stationary Gaussian process  $\mathbf{x} \in \mathbb{R}^p$  with multivariate Gaussian distribution  $\mathcal{N}(0, \Sigma)$  with  $\Sigma$  positive semi-definite. Then the Laplacian matrices corresponding to the family of steady-state equivalent (on  $\mathbf{1}_n^\perp$ ) interaction graphs between the  $p$  variables of  $\mathbf{x}$  are given*



as a function of  $\Psi \in \mathbb{R}^{p \times p}$  projection matrices and  $\kappa \in \mathbb{R}^{p \times p}$  skew-symmetric matrices, by

$$L(\Psi, \kappa) = \Psi(I_p + \kappa)\Sigma^+, \quad (27)$$

where  $\Sigma^+$  denotes the Moore-Penrose pseudo-inverse of  $\Sigma$ .

For the problem of learning GGIMs given a positive semi-definite  $\Sigma$ , we follow a nearly identical approach to Section 5.1 and focus on estimating the Laplacian matrix directly. The associated Lyapunov equation is

$$QLQ^T\bar{\Sigma} + \bar{\Sigma}QLQ^T = 2I_{p-1}, \quad (28)$$

which is linear in  $L$  and can easily be written as a LASSO problem similar to (16). The estimates  $\hat{\Psi}$  and  $\hat{\kappa}$  can be uniquely determined from a directed Laplacian estimate  $\hat{L}$ .

## References

- T. W. Anderson. *An introduction to Multivariate statistical analysis*. John Wiley and Sons, 3 edition, 2003.
- L. Arnold. *Stochastic Differential Equations: Theory and Applications*. Krieger Publishing Company, 1992.
- O. Banerjee, L. E. Ghaoui, and A. d’Aspremont. Model selection through sparse maximum likelihood estimation for multivariate gaussian or binary data. *Journal of Machine Learning Research*, 9:485–516, 2008.
- D. Barber. *Bayesian Reasoning and Machine Learning*. Cambridge University Press, 2012.
- S. Barnett and C. Storey. Analysis and synthesis of stability matrices. *J. Diff. Eq.*, 3:414–422, 1967.
- K. Bollen. *Structure Equations with Latent Variables*. Wiley Publishing, 1989.
- D. M. Chickering. Learning equivalence classes of bayesian-network structures. *Journal of Machine Learning Research*, 2:445–498, 2002.
- K. Fitch. Effective resistance preserving directed graph symmetrization. *SIAM Journal on Matrix Analysis and Applications*, 40(1):49–65, 2019.
- J. Friedman, T. Hastie, and R. Tibshirani. Sparse inverse covariance estimation with the graphical lasso. *Biostatistics*, 9(3):432–441, 2008.
- S. Hassan-Moghaddam, N. K. Dhingra, and M. R. Jovanovic. Topology identification of undirected consensus networks via sparse inverse covariance estimation. In *IEEE 55th Conference on Decision and Control*, pages 4624–4629, 2016.
- T. Hastie, R. Tibshirani, and M. Wainwright. *Statistical Learning with Sparsity: The LASSO and Generalizations*. Chapman and Hall/CRC, 2015.
- Steven M Hill et al. Inferring causal molecular networks: empirical assessment through a community-based effort. *Nature Methods*, 13:310–318, February 2016. URL <https://doi.org/10.1038/nmeth.3773>.

- C. J. Hsieh, I. S. Dhillon, P. K. Ravikumar, and M. A. Sustik. Sparse inverse covariance matrix estimation using quadratic approximation. In *Advances in neural information processing systems 24*, pages 2330–2338, 2011.
- J. D. Kruschwitz, D. List, L. Waller, M. Rubinov, and H. Walter. Graphvar: a user-friendly toolbox for comprehensive graph analyses of functional brain connectivity. *Journal of neuroscience methods*, 245:107–115, 2015.
- S. L. Lauritzen and D. J. Spiegelhalter. Local computations with probabilities on graphical structures and their applications to expert systems. *Journal of the Royal Statistical Society B*, 50(2):157–224, 1988.
- Steffen L. Lauritzen. *Graphical Models*. Clarendon Press, 1996.
- G. Marjanovic and A. O. Hero.  $l_0$  sparse inverse covariance estimation. *IEEE Transactions on Signal Processing*, 63(12):3218–3231, 2015.
- G. Marjanovic and V. Solo. On  $l_q$  optimization and sparse inverse covariance selection. *IEEE Transactions on Signal Processing*, 62(7):1644–1654, 2014.
- Figen Oztoprak, Jorge Nocedal, Steven Rennie, and Peder A Olsen. Newton-like methods for sparse inverse covariance estimation. In *Advances in Neural Information Processing Systems 25*, pages 755–763, 2012.
- K. Sachs, O Perez, D Pe’er, D. A. Lauffenburger, and G. P. Nolan. Causal protein-signaling networks derived from multiparameter single-cell data. *Science*, 308(5721):523–529, 2005.
- N. Souly and M. Shah. Scene labeling using sparse precision matrix. In *IEEE Conference on Computer Vision and Pattern Recognition*, pages 3650–3658, 2016.
- R. S. Varga. On diagonal dominance arguments for bounding  $\|A^{-1}\|_\infty$ . *Linear Algebra and its Applications*, 14:211–217, 1976.
- J. Whittaker. *Graphical Models in Applied Multivariate Statistics*. Wiley Publishing, 2009.
- T. T. Wu and K. Lange. Coordinate descent algorithms for lasso penalized regression. *Annals of Applied Statistics*, 2(224-244), 2008.
- G. F. Young, L. Scardovi, and N. E. Leonard. Robustness of noisy consensus dynamics with directed communication. In *In proc. ACC*, pages 6312–6317, 2010.
- G. F. Young, L. Scardovi, and N. E. Leonard. A new notion of effective resistance for directed graphs—part I: Definition and properties. *IEEE Transactions on Automatic Control*, 61(7):1727–1736, 2016.
- J. Zhang and P. Spirtes. Strong faithfulness and uniform consistency in causal inference. In *Proceedings of Uncertainty in Artificial Intelligence*, pages 632–639, 2003.
- W. Zhang and P. Fung. Sparse inverse covariance matrices for low resource speech recognition. In *IEEE Transactions on Audio, Speech, and Language Processing*, pages 659–668, 2013.